Journal of Biotechnology 142 (2009) 97–106

Contents lists available at ScienceDirect

Journal of Biotechnology

journal homepage: www.elsevier.com/locate/jbiotec

Pyranose 2-oxidase from *Phanerochaete chrysosporium*—Expression in *E. coli* and biochemical characterization

Ines Pisanelli[a], Magdalena Kujawa[a,d], Oliver Spadiut[a], Roman Kittl[a,d], Petr Halada[b], Jindrich Volc[b], Michael D. Mozuch[c], Philip Kersten[c], Dietmar Haltrich[a], Clemens Peterbauer[a,*]

[a] *Department of Food Sciences and Technology, BOKU, University of Natural Resources and Applied Life Sciences, Vienna, Austria*
[b] *Institute of Microbiology, Academy of Sciences of the Czech Republic, Prague, Czech Republic*
[c] *Forest Products Laboratory, Forest Service, U.S. Department of Agriculture, Madison, WI, USA*
[d] *Research Center Applied Biocatalysis, Graz, Austria*

ARTICLE INFO

Article history:
Received 22 September 2008
Received in revised form 2 February 2009
Accepted 23 March 2009

Keywords:
Pyranose 2-oxidase
Phanerochaete chrysosporium
Lignocellulose degradation
Heterologous expression

ABSTRACT

The presented work reports the isolation and heterologous expression of the *p2ox* gene encoding the flavoprotein pyranose 2-oxidase (P2Ox) from the basidiomycete *Phanerochaete chrysosporium*. The *p2ox* cDNA was inserted into the bacterial expression vector pET21a(+) and successfully expressed in *Escherichia coli*. We obtained active, fully flavinylated recombinant P2Ox in yields of approximately 270 mg/l medium. The recombinant enzyme was provided with an N-terminal T7-tag and a C-terminal His_6-tag to facilitate simple one-step purification. We obtained an apparently homogenous enzyme preparation with a specific activity of 16.5 U/mg. Recombinant P2Ox from *P. chrysosporium* was characterized in some detail with respect to its physical and catalytic properties, both for electron donor (sugar substrates) and – for the first time – alternative electron acceptors (1,4-benzoquinone, substituted quinones, 2,6-dichloroindophenol and ferricenium ion). As judged from the catalytic efficiencies k_{cat}/K_m, some of these alternative electron acceptors are better substrates than oxygen, which might have implications for the proposed *in vivo* function of pyranose 2-oxidase.

1. Introduction

Pyranose 2-oxidase (P2Ox, pyranose:oxygen 2-oxidoreductase; EC 1.1.3.10) belongs to the glucose–methanol–choline (GMC) oxidoreductase family of flavin adenine dinucleotide (FAD)-dependent sugar oxidoreductases (Hallberg et al., 2004). It is localized in the periplasmic space and associated with membranous materials of lignocellulolytic fungi (Daniel et al., 1992) and is believed to play a role in lignocellulose degradation by providing the essential co-substrate hydrogen peroxide for lignin and manganese peroxidases (Daniel et al., 1994). Another biological function under discussion is its role in a secondary metabolic pathway leading from D-glucose via 2-keto-D-glucose to the β-pyrone-antibiotic cortalcerone (Baute et al., 1977). In general, pyranose 2-oxidase is a 270 kDa homotetramer that catalyzes regioselectively the C-2 oxidation of several aldopyranoses to the respective 2-dehydro derivates, transferring electrons to molecular oxygen to yield H_2O_2. However, for some substrates, the enzyme also displays specificity for oxidation at C-3 (Freimund et al., 1998; Giffhorn, 2000; Eriksson et al., 1986). P2Ox can also transfer electrons to acceptors other than oxygen, e.g., quinones, organic radical molecules or complexed metal ions, but this property has not been studied and compared in any detail for different enzymes (Shin et al., 1993).

Pyranose 2-oxidase is an enzyme with high potential for biotransformations of carbohydrates; applications in bioprocesses, clinical analytics and in synthetic carbohydrate chemistry have been reviewed (Giffhorn, 2000). Recently, we showed that P2Ox can be electrically wired to graphite electrodes in the presence of suitable osmium redox polymers, and hence could be used advantageously in enzyme electrodes or biofuel cells (Tasca et al., 2007).

A critical point in enzymatic processes is the availability of the biocatalyst and its stability under operational conditions. Production of native enzymes by fungal cultures is often – depending on the source – hampered by slow growth and limited yield. Heterologous expression in a suitable recombinant strain offers an attractive alternative with higher yields, shorter fermentation times and often cheaper fermentation media. Techniques such as site-directed mutagenesis, directed evolution, gene shuffling and combinations of these methods have been shown to be powerful

* Corresponding author at: Department für Lebensmittelwissenschaften und –technologie, Universität für Bodenkultur, Muthgasse 18, A-1190 Wien, Austria. Tel.: +43 1 36006 6274; fax: +43 1 36006 6251.
E-mail address: clemens.peterbauer@boku.ac.at (C. Peterbauer).
URL: http://www.dlwt.boku.ac.at/400.html (C. Peterbauer).

0168-1656/$ – see front matter © 2009 Elsevier B.V. All rights reserved.
doi:10.1016/j.jbiotec.2009.03.019

tools for enzyme engineering and protein design (Bornscheuer and Pohl, 2001). All of these methods require heterologous expression of the respective encoding gene, with *Escherichia coli* and yeast-based systems being the preferred choice whenever possible due to short generation times, ease of handling and amenability for genetic engineering.

There are several examples of pyranose 2-oxidase genes from basidiomycetous fungi cloned and expressed heterologously, all in *E. coli*-based expression systems. These include *Coriolus* (*Trametes*) *versicolor* (Nishimura et al., 1996), *Trametes hirsuta* (Christensen et al., 2000), *Tricholoma matsutake* (Takakura and Kuwata, 2003), *Peniophora* sp. (Bannwarth et al., 2004), *Trametes multicolor* (synonymous for *T. ochracea*) (Kujawa et al., 2006; Vecerek et al., 2004) and *Trametes pubescens* (Maresova et al., 2005). Experimentally determined crystal structures of P2Ox are available for only two proteins to date, those from *T. multicolor* (Hallberg et al., 2004) and *Peniophora* sp. (Bannwarth et al., 2004), which have highly similar amino acid sequences. In addition, the structures of P2Ox liganded either with the poor substrate 2-deoxy-2-fluoro-D-glucose or its product 2-keto-D-glucose are published (Bastian et al., 2005; Kujawa et al., 2006).

Phanerochaete chrysosporium is considered the prime model organism among white-rot fungi for lignin degradation and investigation of the respective enzyme systems; its genome was recently sequenced and annotated by the US Department of Energy Joint Genome Initiative (Martinez et al., 2004). The biochemistry and transcriptional regulation of pyranose 2-oxidase from this fungus (PcP2Ox) is reported (Artolozaga et al., 1997; De Koker et al., 2004; Eriksson et al., 1986). A comparison of P2Ox sequences reveals several distinct features in the sequences of the enzymes from *P. chrysosporium*, as well as from *Lyophyllum shimeji* and *T. matsutake*, when compared to those from *Trametes* spp. and *Peniophora* spp., namely deviations from consensus in the first and second FAD-binding subregions (De Koker et al., 2004). PcP2Ox further deviates from consensus in the third FAD-binding subregion. These differences are reflected in the phylogenetic relationship of P2Ox sequences, with the *P. chrysosporium* and the *L. shimeji* sequences grouping in a separate clade from *Trametes* spp. and *Peniophora* spp. Structural investigations of *P. chrysosporium* P2Ox could therefore provide valuable insight into structure-function relationships of GMC oxidoreductases, yet crystallization of wild-type fungal P2Ox from *P. chrysosporium* is unsuccessful to date, probably due to microheterogeneity of the wild-type enzyme preparations reported (Artolozaga et al., 1997; De Koker et al., 2004). Heterologous expression will also be an invaluable help to produce enzyme variants for further detailed studies.

Here we report the successful heterologous expression of PcP2Ox in *E. coli*. Biochemical characterization shows similarity with the reported properties of the wild-type protein for electron-donor sugar substrates, while activity with alternate electron acceptors, in addition to oxygen, is reported for the first time. Enzyme kinetics with benzoquinone suggests a possible role for PcP2Ox in redox cycling during lignocellulose metabolism.

2. Materials and methods

2.1. Chemicals

Chemicals used in this study were of the purest grade available and were purchased from Sigma (St. Louis, MO) unless otherwise stated. Horseradish peroxidase (grade II; EC 1.11.1.7) was obtained from Roche (Mannheim, Germany), various electron acceptors were provided from Aldrich (Steinheim, Germany), and bovine serum albumin (BSA) was from United States Biochemical (Cleveland, OH). Restriction endonucleases, T4 DNA ligase and DNA modifying enzymes were obtained from Promega (Madison, WI).

2.2. Organisms, plasmids and media

E. coli strain DH5α was used for cloning experiments and plasmid propagation. *E. coli* strain BL21(DE3) (Novagen, Madison, WI) was used as a host for the production of the active P2Ox. Plasmid pGEM-T Easy (Promega) was used for cloning of PCR fragments, and the expression vector pET21a(+) (Novagen) for recombinant production of P2Ox.

Production of recombinant PcP2Ox was done in the following media: Luria-Bertani (LB; (Ausubel et al., 1990)), 2× LB, Terrific Broth (TB; Ausubel et al., 1990), and MCHGly medium containing (g/l): glycerol, 10; casein hydrolysate, 10; $Na_2HPO_4{\cdot}12H_2O$, 14.6; KH_2PO_4, 3.0; NaCl, 0.5; NH_4Cl, 1.0; and $MgSO_4{\cdot}7H_2O$, 0.25. Isopropyl-β-D-thiogalactopyranoside (IPTG) or lactose in different concentrations was added to induce the expression system.

2.3. Isolation and expression of P2Ox-encoding cDNA

The cDNA sequence encoding P2Ox of *P. chrysosporium* BKM-F-1767 (GenBank accession no. AY522922 (De Koker et al., 2004) was used to construct the expression vector. Isolation of mRNA and first strand synthesis were carried out as described by Stewart and Cullen (1999) using the primers 5′-CGGAGTCAGAGGACTGCTCCA-3′ and 5′-ATTGTACTTACGCAGCACGAGGTT-3′ (forward and reverse, respectively; mRNA provided by Dan Cullen and Jill Gaskell of Forest Products Laboratory, Madison WI, and assistance with first strand synthesis is gratefully acknowledged). The *p2ox*-coding sequence was amplified using two modified primers based on the genomic sequence: poxMK1for: 5′-CGC**GGATCC**ATGTTTCTTGACACCACACCA-3′; and poxMK1rev: 5′-CAG**AAGCTT**GCCGCGGTGACGACCAAA-3′ containing BamHI (poxMK1for) and HindIII (poxMK1rev) restriction sites, respectively (bold print), to facilitate subsequent insertion into the expression vector.

The PCR reaction mixture contained 34 μl sterile nanopure water, 5 μl 10× Pfu buffer (Promega), 4 μl 2.5 mM dNTPs (2.5 mM each), 1 μl template cDNA, 3 μl of each primer (10.5 pmol/l) and 0.5 μl Pfu proofreading thermostable DNA polymerase (Promega).

The resulting PCR product of approximately 1.9 kb was purified from an agarose gel using the Wizard SV Gel & PCR CleanUp System and ligated into a pGEM-T Easy Vector (both from Promega). The A-tailing procedure, ligation and transformation into *E. coli* DH5α were performed according to the manufacturer's recommendation. After sequence analysis, the *p2ox* cDNA insert was isolated by digestion with BamHI and HindIII and ligated into the respective sites of pET21a(+) (Novagen) in frame with the N-terminal T7-tag and C-terminal His_6-tag encoded by the expression vector. *E. coli* strain BL21(DE3) was the host for expression of the resulting plasmid for protein production.

Several clones were grown overnight at 37 °C in 5 ml LB medium with 100 μg/ml of ampicillin, the cell pellet after centrifugation was resuspended in Start Buffer (20 mM bis–tris buffer, 1 M NaCl, and 10 mM imidazole, pH 6.4), and homogenized using a French press at 100 MPa. The cell homogenate was tested for presence of pyranose oxidase activity. Cultivation on a larger scale to provide material for biochemical characterization was done in 1-l shake flasks. Twenty-five milliliter TB medium supplemented with 100 μg/ml of ampicillin were inoculated with a single colony, and cultivated at 37 °C and 150 rpm for 6 h. TB medium (225 ml) containing 100 μg/ml of ampicillin was inoculated with this starter culture and cultivated for additional 2 h, then lactose was added to a final concentration of 5 g/l. After overnight cultivation at 25 °C and 150 rpm, the cells were harvested by centrifugation at 10,000 × *g* for 20 min and 4 °C. The cell pellet was suspended in start buffer and homogenized in a French press. The homogenate was centrifuged at 30,000 × *g* for

30 min and 4 °C, and the supernatant was recovered as a crude extract.

2.4. Enzyme purification

recP2Ox was purified by one-step immobilized metal affinity chromatography (IMAC), on a column (40 ml) packed with Profinity IMAC Ni-Charged Resin (Bio-Rad Inc., Hercules, CA) specific for recombinant His-tagged proteins. The column was pre-equilibrated with start buffer (see above), and the crude extract was applied to the column at a rate of 2.5 ml/min. After an additional washing step with Start Buffer (two column volumes) the enzyme was eluted at a rate of 2.5 ml/min by using a linear gradient (0–1 M imidazole in Start Buffer) in 10 column volumes. Active fractions (10 ml each, a total of 70 ml) were pooled, desalted and concentrated in 50 mM potassium phosphate buffer (pH 6.5) using Amicon Ultra Centrifugal Filter units (Millipore, Billerica, MA), filter sterilized, and stored at 4 °C.

2.5. Enzyme assay

Unless otherwise specified, pyranose oxidase activity was determined spectrophotometrically at 420 nm and 30 °C by measuring the formation of H_2O_2 for 3 min with a peroxidase-coupled assay using ABTS [2,2′-azinobis(3-ethylbenzthiazolinesulfonic acid)] (ε_{420} = 43,200 M^{-1} cm^{-1}) as the chromogen. The standard assay mixture (total volume 1 ml) contained 1 μmol of ABTS in 50 mM potassium phosphate buffer (pH 6.5), 2 U of horseradish peroxidase, 100 μmol of D-glucose, and a suitable amount of P2Ox sample. One unit of P2Ox activity was defined as the amount of enzyme necessary for oxidation of 2 μmol of ABTS (equivalent to the oxidation of 1 μmol of D-glucose) per minute under the conditions described above (Danneel et al., 1992). Protein contents were determined by the dye-binding method of Bradford, using BSA as the standard.

The effect of pH on different electron acceptors was determined using the following buffers: sodium citrate (pH 3.0–6.0), potassium phosphate (pH 5.5–8.0), Tris–HCl (pH 7.5–9), sodium phosphate (pH 10–12), and sodium borate (pH 8.0–12), each at 100 mM.

2.6. Electrophoretic analysis

Polyacrylamide gel electrophoresis (PAGE) as well as isoelectric focusing was done on a PhastSystem unit (Pharmacia LKB/GE Healthcare Life Sciences, Uppsala, Sweden) according to the manufacturer's instructions. Protein bands were visualized by silver staining. The native molecular mass of the enzyme was estimated in 8–25% gradient gels under nondenaturing conditions using a high-molecular-mass protein standard (Amersham, Piscataway, NJ). Subunit molecular mass was determined by sodium dodecyl sulfate (SDS)-PAGE and the low-molecular-mass protein kit (Amersham) as a standard. The marker mix used in isoelectric focusing was for a range of 3.6–6.6 (Sigma).

2.7. Cofactor characterization

FAD absorption spectra were recorded using an 8453 UV–visible Spectrophotometer (Agilent Technologies, Santa Clara, CA) with diode array detection at room temperature. The enzyme was reduced by the addition of D-glucose (20 mM). Homogeneously purified P2Ox was treated with 5% trichloroacetic acid at 100 °C for 10 min; denatured protein was removed by centrifugation and the presence of liberated flavin was measured in the supernatant at 450 nm.

2.8. N-terminal sequencing

The N-terminal sequencing of P2Ox using Edman degradation chemistry was performed on a Procise protein sequencer (Applied Biosystems, Foster City, CA) according to the manufacturer's manual.

2.9. Enzymatic in-gel digestion

CBB-stained protein bands were excised from the gel, cut into small pieces and washed with 10 mM DDT, 0.1 M 4-ethylmorpholine acetate (pH 8.1) in 50% acetonitrile (MeCN). After destaining, the proteins were reduced with 30 mM tris(2-carboxyethyl)phosphine hydrochloride (TCEP) at 65 °C for 30 min and alkylated by 30 mM iodoacetamide for 60 min in the dark. The gel pieces were further washed with water, shrunk by dehydration in MeCN and reswollen in water. The supernatant was removed and the gel partly dried in a SpeedVac concentrator. The gel pieces were then reconstituted in a cleavage buffer containing 0.01% 2-mercaptoethanol, 0.1 M 4-ethylmorpholine acetate, 10% MeCN and sequencing grade trypsin (20 ng/μl; Promega) or Asp-N protease (10 ng/μl; Roche). After overnight digestion, the resulting peptides were extracted to 40% MeCN/0.1% TFA.

2.10. MALDI-TOF mass spectrometry

A solution of α-cyano-4-hydroxycinnamic acid (Sigma) in aqueous 50% MeCN//0.1% TFA (5 mg/ml) was used as a MALDI matrix. The sample (0.5 μl) was deposited on the MALDI target and allowed to air-dry at room temperature. After complete evaporation, 0.5 μl of the matrix solution was added. MALDI mass spectra were measured on an Ultraflex III instrument (Bruker Daltonics, Bremen, Germany) equipped with a smartbeam solid-state laser and LIFT technology for MS/MS analysis. The spectra were acquired in the mass range of 700–5000 Da and calibrated internally using the monoisotopic $[M+H]^+$ ions of autoproteolytic fragments of trypsin (842.5 and 2211.1 Da).

2.11. Steady-state kinetic measurements

Unless otherwise stated, all measurements were performed at 30 °C in 50 mM potassium phosphate buffer (pH 6.5). Measurements of kinetic constants for various electron donors (sugar substrates) were done with oxygen (air saturation) as electron acceptor and the routine ABTS-peroxidase assay performed as described above. Kinetic constants for various electron acceptors were determined using 20 mM D-glucose as the electron donor, and measurements were performed at the pH optimum of the respective acceptor as well as at pH 6.5. The kinetic constants for the electron acceptors 1,4-benzoquinone, 2,6-dichloroindophenol (DCIP), and the ferricenium Fc^+ ion (using ferricenium hexafluorophosphate $Fc^+PF_6^-$ (Aldrich, Steinheim, Germany)) were measured as previously described (Kujawa et al., 2007). In short, 10 μl of appropriately diluted enzyme was added to 990 μl of the appropriate buffer containing the sugar substrate D-glucose and which had been flushed with nitrogen for the removal of oxygen. 1,4-Benzoquinone was varied from 0.01 to 2.0 mM, and the absorbance change at 290 nm (ε = 2.24 mM^{-1} cm^{-1}) was followed for 180 s. DCIP was varied from 0.01 to 0.3 mM, and the absorbance change was measured at 520 nm (ε = 6.8 mM^{-1} cm^{-1}) for 180 s. $Fc^+PF_6^-$ was varied from 0.005 to 1.0 mM, and the absorbance change at 300 nm (ε = 4.3 mM^{-1} cm^{-1}) was followed for 180 s. All kinetic constants were calculated by non-linear least-squares regression, fitting the observed data to the Henri–Michaelis–Menten equation. Turnover numbers (k_{cat}) and catalytic efficiencies (k_{cat}/K_m) were

Table 1
Purification of recombinant P2Ox from *Phanerochaete chrysosporium* by immobilized metal affinity chromatography (IMAC).

Purification step	Total protein (mg)	Total activity (U)	Specific activity (U/mg)	Recovery (%)	Purification (fold)
Crude extract	1260	3490	2.77	100	1
IMAC	161	2660	16.5	76.2	5.96

calculated using a molecular mass of 65 kDa for the P2Ox subunit.

3. Results

3.1. Isolation and heterologous expression of P2Ox-encoding cDNA

A full length cDNA encoding pyranose oxidase (P2Ox) from *P. chrysosporium* (GenBank accession number AY522922 (De Koker et al., 2004)) was successfully expressed in *E. coli* BL21(DE3). The nucleotide sequence contains an open reading frame of 1,863 bp encoding a polypeptide of 621 amino acids. Based on the cDNA sequence, two modified oligonucleotide primers containing restriction sites for in-frame ligation of the gene into pET21a(+) were designed. These primers were used to re-amplify the cDNA and construct the expression vector containing *p2ox* cDNA under the control of a lactose- or IPTG-inducible T7 promoter fused in frame with the N-terminal T7-tag as well as a C-terminal His_6-tag encoded by the vector. The resulting vector was transformed into the production strain BL21(DE3), and ampicillin-resistant clones were tested for the presence of P2Ox activity after small-scale cultivation. The bacterial clone with the highest activity (1.11 U/mg) was selected for further studies.

Recombinant P2Ox production by *E. coli* BL21(DE3) was done in LB, 2× LB, TB and MCHGly medium. Specific activities of 2.22 U/mg (using IPTG with a final concentration of 0.1 mM) and 1.66 U/mg (IPTG final concentration 1 mM), respectively, were obtained on TB and MCHGly medium, while specific activities on LB and 2xLB medium were significantly lower (data not shown). Routinely, approx. 270 mg/l (as calculated from 4500 U/l and a specific activity of 16.5 U/mg) of active, soluble recombinant P2Ox were obtained in shake-flask cultivations under the growth conditions outlined above.

3.2. Enzyme purification

A typical purification procedure of recP2Ox from *P. chrysosporium* is summarized in Table 1. The enzyme was purified six-fold from the crude extract with a yield of 76% and a specific activity of 16.5 U/mg under standard assay conditions when glucose and oxygen (air) were used as substrates. The one-step purification procedure yielded an apparently homogenous protein, as judged by SDS-PAGE (Fig. 1).

3.3. Physical properties

The molecular mass of native recombinant P2Ox was approximately 250 kDa as estimated by PAGE under non-dissociating conditions (Fig. 2). SDS-PAGE of recP2Ox resulted in a single band at 65 kDa (Fig. 1), indicating a homotetrameric structure of the active enzyme, as was described for pyranose oxidase from the fungal wild-type as well as for the enzymes from other sources. Isoelectric focusing under native conditions showed a major band of p*I* 5.2 and two minor isoforms of recP2Ox ranging from p*I* 5.1 to 5.3 (Fig. 3).

Purified recP2Ox was bright yellow and produced a typical flavoprotein spectrum with absorption maxima at 357 and 459 nm. When the enzyme was reduced by addition of glucose in the absence of oxygen, the peak at 459 nm disappeared (Fig. 4). Treat-

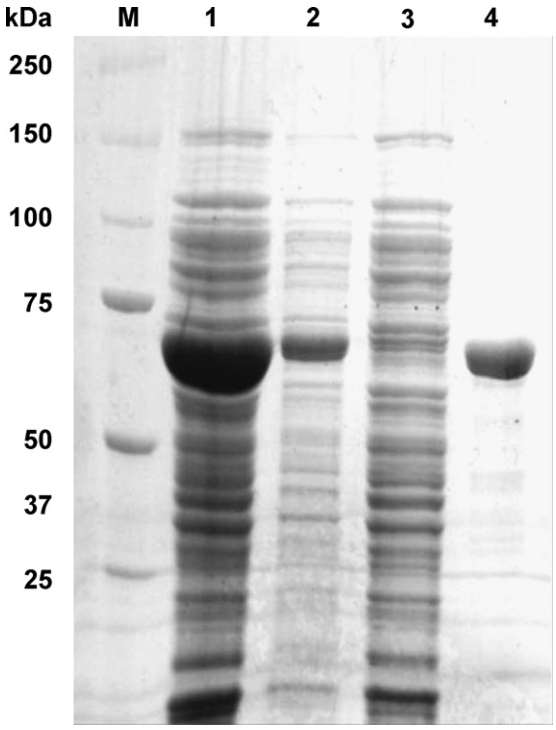

Fig. 1. SDS-PAGE analysis of rP2Ox from *P. chrysosporium*. Lane M, low-molecular-mass protein standards, Amersham; lane 1, crude cell extract undiluted; lane 2, crude cell extract diluted 1:10; lane 3, flow-through from IMAC; lane 4, purified pyranose oxidase after IMAC.

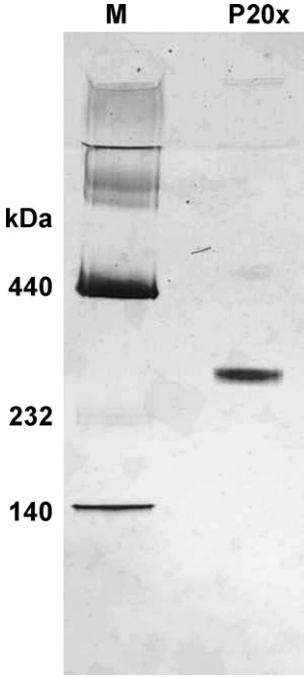

Fig. 2. Native PAGE analysis of rP2Ox from *P. chrysosporium*. Lane M, high-molecular-mass marker protein kit, Amersham; rP2Ox, purified recombinant pyranose oxidase.

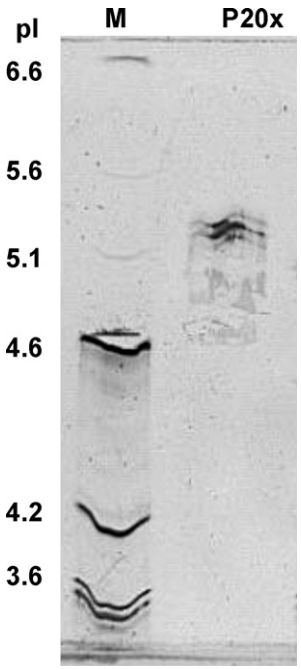

Fig. 3. Isoelectric focusing of rP2Ox from *P. chrysosporium*. Lane M, isoelectric marker range 3.6–6.6 (Sigma); rP2Ox, purified recombinant pyranose 2-oxidase.

ment of the enzyme with 5% trichloroacetic acid at 100 °C for 10 min did not release the flavin moiety from the polypeptide, suggesting a covalent linkage to the protein.

3.4. N-terminus

The N-terminus of the purified protein was determined using Edman-chemistry and was found to be MASMTGGQQMG, the sequence of the vector-encoded T7-tag. However, an additional protein was also detected as secondary peaks in the sequencing runs (not shown). This protein represented approx. 15% of the total amount, and the sequence was that of the theoretical translation of the P2Ox cDNA (MFLDTTPFRAD). MS/MS peptide sequencing of the digested purified protein samples gave sequence coverages of 63% (Trypsin) and 50% (AspN protease), respectively, with a total coverage of 77%. The only sequences not belonging to the translation of the P2Ox cDNA could be assigned to the T7-tag.

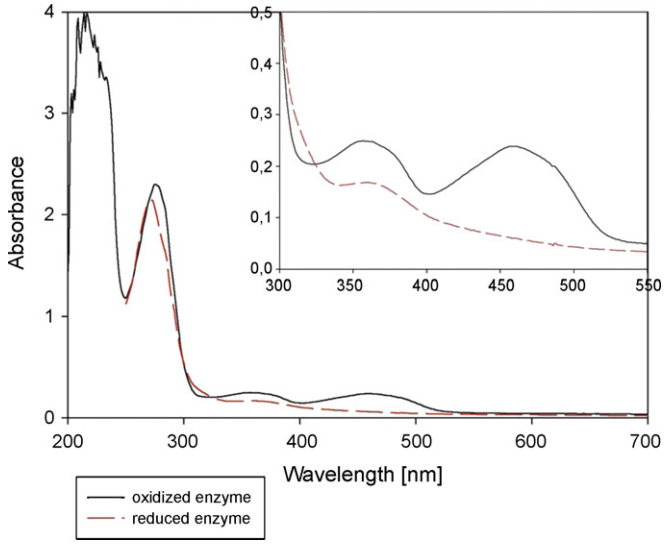

Fig. 4. FAD absorption spectrum. The spectrum of the oxidized enzyme displays maxima at 357 and 459 nm (black line). In the reduced enzyme, the 459 nm maximum disappears (red interrupted line). (For interpretation of the references to colour in this figure legend, the reader is referred to the web version of the article.)

3.5. pH dependence of activity

pH optima for the purified recombinant P2Ox were determined for the electron acceptors oxygen, 1,4-benzoquinone, the ferricenium ion (Fc^+), and 2,6-dichloroindophenol (DCIP). The enzyme exhibited rather sharp pH profiles for Fc^+ and DCIP with pH optima of 8.0 and 6.5, respectively. When Fc^+ was the electron acceptor we found a strong dependence of activity on the buffer used and that P2Ox retained 60% of its maximal activity even at pH 9.5. Bell-shaped profiles with an optimum pH range between 6.0 and 9.0 were observed when oxygen was used as the electron acceptor while 1,4-benzoquinone displayed an even broader range from pH 4.0 to 9.0 (Fig. 5).

3.6. Kinetic properties

Various sugars were tested as possible substrates of recP2Ox, and the activities relative to those with D-glucose were determined under standard assay conditions at a sugar substrate concentration of 100 mM. The enzyme showed approximately 30% relative activity with L-sorbose and D-xylose and 5% relative activity with D-galactose, while D-fructose was hardly oxidized at all. Subsequently, the kinetic constants were determined for these sugars using oxygen (air) as electron acceptor (Table 2). The highest catalytic efficiency (k_{cat}/K_m) was found for D-glucose (98.9 $mM^{-1}\ s^{-1}$) whereas the corresponding values for L-sorbose, D-xylose, and D-galactose were ~40–50-fold lower (Table 2). The lowest catalytic efficiency was measured for D-fructose as a substrate as a result of both an unfavourable Michaelis constant K_m and turnover number k_{cat}.

In addition to oxygen, recP2Ox from *P. chrysosporium* is able to transfer electrons to other acceptors. Kinetic constants were determined for the two-electron acceptors 1,4-benzoquinone, various substituted quinones and DCIP as well as for one-electron acceptors, including the ferricenium ion Fc^+ or the ABTS cation radical. These measurements were performed with D-glucose as the saturating substrate and both at the pH value of the standard assay, pH 6.5, and at the pH optimum of the respective electron acceptor substrates (benzoquinone, pH 4.5; DCIP, pH 6.5; Fc^+, pH 8.0). Results are summarized in Table 3. 1,4-Benzoquinone shows a k_{cat}/K_m value of ~$10^7\ M^{-1}\ s^{-1}$ when the reaction is carried out at pH 4.5 while at pH 6.5 the value is reduced to about one third of this value (Table 3); this is mainly the effect of a considerably increased Michaelis constant at the higher pH value. Variously substituted 1,4-benzoquinones showed K_m values comparable to that of 1,4-benzoquinone, whereas the turnover numbers determined for these substrates were decreased dramatically. The pH optimum for DCIP was found to be similar to the standard assay conditions. DCIP as an electron acceptor of *Pc*P2Ox is characterized by a very low Michaelis constant in the micromolar range, but also by k_{cat} values that are significantly lower than that of, e.g., 1,4-benzoquinone. P2Ox showed significant activity with several one-electron acceptors. For Fc^+ the pH of the reaction does not affect the K_m value significantly, while at the optimal pH of 8.0 and in the presence of borate buffer the turnover number is increased 2.4-fold compared to pH 6.5, resulting in an ~3-fold higher catalytic efficiency ($1.9 \times 10^6\ M^{-1}\ s^{-1}$). In comparison, the catalytic efficiency for the other one-electron acceptors tested, the ABTS cation radical and ferricyanide, were considerably lower.

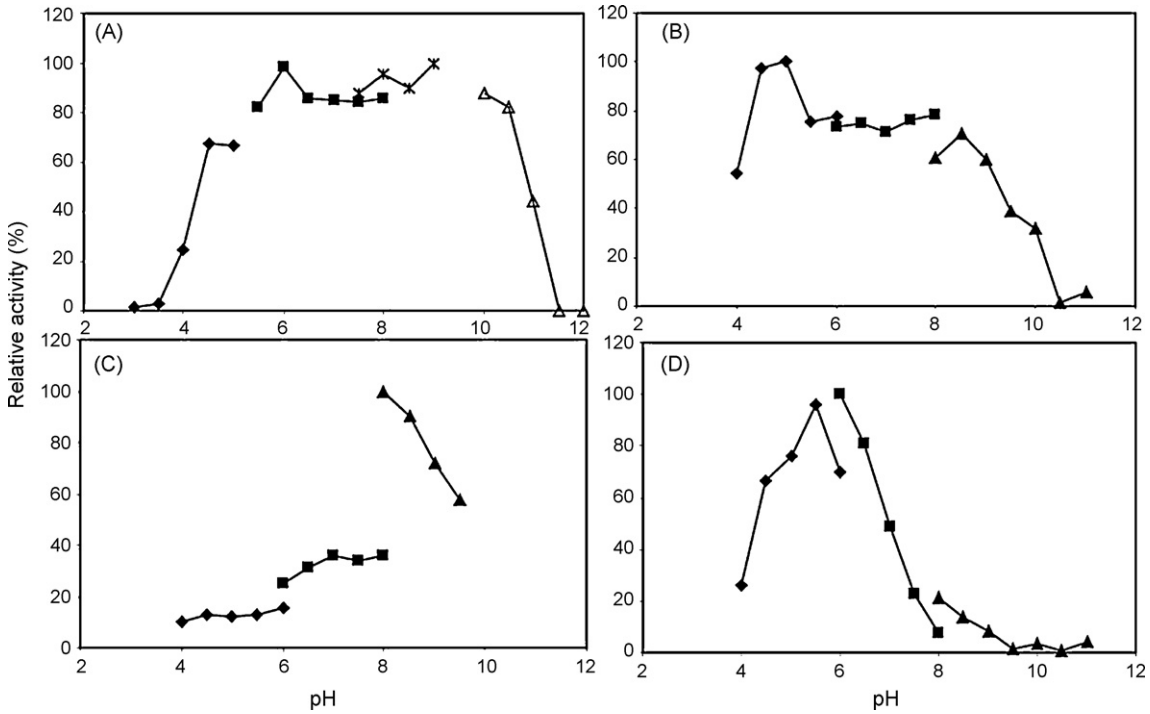

Fig. 5. Effect of pH on the activity of recP2Ox from *P. chrysosporium* in the presence of different electron acceptors. (A) Oxygen, (B) 1,4-benzoquinone, (C) ferricenium ion, and (D) 2,6-dichloroindophenol. The buffers used were 100 mM sodium citrate (♦), 100 mM potassium phosphate (■), 100 mM borate (▲), 100 mM Na_3PO_4 (△), 100 mM Tris–HCl (*).

Table 2
Apparent steady-state kinetic constants of recombinant pyranose 2-oxidase from *P. chrysosporium* kinetic constants were determined for several electron donors at 30 °C by using oxygen (air saturation) as electron acceptor under the standard ABTS assay conditions.

Substrate	v_{max} (μmol min^{-1} mg^{-1})	K_m (mM)	k_{cat} (s^{-1})	k_{cat}/K_m (mM^{-1} s^{-1})
D-Glucose	19.9 ± 0.74	0.84 ± 0.15	83.1 ± 3.1	98.9
L-Sorbose	14.1 ± 0.81	23.5 ± 3.4	58.8 ± 3.4	2.50
D-Xylose	10.8 ± 0.48	20.9 ± 2.7	44.9 ± 2.0	2.15
D-Galactose	1.17 ± 0.03	2.94 ± 0.35	4.87 ± 0.13	1.66
D-Fructose	0.45 ± 0.068	103 ± 46	1.88 ± 0.28	0.0183

4. Discussion

We report here on the successful expression in *E. coli* of a *P. chrysosporium* cDNA encoding pyranose 2-oxidase, as well as its biochemical and kinetic characterization. The respective gene had previously been identified in the *P. chrysosporium* genome as encoding the P2Ox enzyme purified from mycelium grown on wheat bran supplemented with corn steep liquor (De Koker et al., 2004). cDNA was synthesized from mRNA obtained under carbon-limiting conditions, as this was shown to promote transcription of the *p2ox*-gene (De Koker et al., 2004), and ligated into an expression plasmid for *E. coli*, a host–vector system that was already shown to work effectively for other, related pyranose oxidase enzymes (Bastian et al., 2005; Heckmann-Pohl et al., 2006; Kotik et al., 2004; Maresova et al., 2005; Takakura and Kuwata, 2003). We were able to obtain yields of 4500 U of P2Ox activity and 270 mg of active P2Ox protein per liter of production medium in shake-flask cultures without optimization of the expression system and cultivation conditions. This is significantly higher than the yields reported thus far for P2Ox from, e.g., *Trametes* spp., which typically range from 50 to 100 mg/l (Kotik et al., 2004; Maresova et al., 2005), or *Peniophora gigantea*

Table 3
Apparent kinetic constants of recP2Ox from *P. chrysosporium* for several electron acceptors Kinetic constants were determined at 30 °C by using 20 mM D-glucose as electron donor under standard assay conditions (pH 6.5) unless otherwise indicated.

Electron acceptor	v_{max} (μmol min^{-1} mg^{-1})	K_m (mM)	k_{cat} (s^{-1})	k_{cat}/K_m (mM^{-1} s^{-1})
Oxygen (pH 8.0)[a]	26.1 ± 0.2	1.22 ± 0.02	109 ± 0.8	89.2
1,4-Benzoquinone	96 ± 3.5	0.11 ± 0.01	400 ± 14	3640
1,4-Benzoquinone (pH 4.5)	115 ± 8.7	0.042 ± 0.013	477 ± 36	11900
$Fc^+PF_6^-$[b]	54.8 ± 35.8	0.33 ± 0.35	228 ± 149	691
$Fc^+PF_6^-$ (pH 8.0)	132 ± 8.6	0.29 ± 0.05	549 ± 36	1890
DCIP[c]	25.9 ± 3.9	0.051 ± 0.031	108 ± 16	2150
2-Chloro-1,4-benzoquinone	0.037 ± 0.004	0.31 ± 0.08	0.15 ± 0.02	0.48
2-Methoxy-1,4-benzoquinone	9.65 ± 0.76	0.21 ± 0.05	40.1 ± 3.16	191
2-Methyl-1,4-benzoquinone	0.029 ± 0.001	0.51 ± 0.05	0.12 ± 0.004	0.23
Ferricyanide	0.074 ± 0.046	3.43 ± 2.51	0.30 ± 0.19	0.087
2,6-Dimethyl-1,4-benzoquinone	2.09 ± 0.32	1.59 ± 0.34	8.69 ± 1.33	5.46
Tetrafluoro-1,4-benzoquinone	1.59 ± 0.16	0.64 ± 0.16	6.61 ± 0.66	10.3
ABTS cation radical	0.32 ± 0.061	0.09 ± 0.044	1.33 ± 0.25	13.4

[a] Data taken from Artolozaga et al. (1997); measured at pH 8.0 and 25 °C in the presence of 100 mM D-glucose.
[b] $Fc^+PF_6^-$, ferricenium hexafluorophosphate.
[c] DCIP, 2,6-dichloroindophenol.

reported at 170 mg/l (Bastian et al., 2005). It can be expected that the use of a bioreactor and an optimized fermentation protocol can substantially improve upon these yields of *Pc*P2Ox, which will make a large-scale industrial production of this enzyme feasible. Furthermore, experiments to obtain high-quality protein crystals for X-ray-structure determination, which were unsuccessful thus far, would no longer be hampered by limited availability of pure protein.

The protein was expressed with both the N-terminal T7-tag as well as the C-terminal His-tag. Previous experience with P2Ox from *T. multicolor/ochracea* has shown that Ni-based affinity chromatography resins may leak Ni ions into the eluate, which has a detrimental effect on enzyme activity (our unpublished information). An overnight incubation in a buffer containing 100 mM EDTA followed by a buffer exchange can remedy that, but may also lead to enzyme loss. Therefore the T7-tag was added as well, in order to provide a possible alternative for detection and purification. The translational fusion with T7 may also be reason for the high levels of protein production; the tag is derived from the most abundant phage T7 gene product (Stevens, 2000).

MS/MS peptide sequencing of the recombinant *Pc*P2Ox expressed in *E. coli* gave 77% sequence coverage in total, indicating that the protein expressed and purified indeed corresponds to the proposed *p2ox* gene. In addition, no peptide sequences not belonging to the P2Ox-encoding gene were discovered with the exception of a short sequence region that could be assigned to the T7-tag. When the N-terminal sequence was determined by Edman degradation of the purified protein, it was found that a fraction of the sample, estimated to approximately 15% of the total, did not contain the vector-encoded T7-tag preceding the coding sequence, but started with the methionine of the original cDNA (Met-1). Presumably, the encoding ATG is also used – to a certain degree – as an alternative translational start point. Proteins that are translated from this start codon, however, also possess the C-terminal His_6-tag, which was used for the one-step-purification of the recombinant protein, and are therefore co-purified. Use of affinity chromatography employing antibodies against the T7-tag may avoid this co-purification of the fraction missing the T7-tag. The two ATGs contained in the sequence encoding the T7-tag apparently are not used as an alternative start codon, or if so, only to such a minor fraction as to be undetectable in the N-terminal sequencing. The difference of only 12 amino acids between the two proteins did not result in a sufficiently altered electrophoretic mobility to be detected in SDS-PAGE as only one sharp band was observed for the purified sample, but may account for the observed minor bands in isoelectric focusing, especially since this short tag contains one charged amino acid and the His_6-tag contains additional charged residues. The phenomenon of several distinct bands was observed for the native protein purified from the original source, where doublet bands were observed on SDS-PAGE as well as microheterogeneity in isoelectric focusing (De Koker et al., 2004; Volc and Eriksson, 1988), but the reason for this remains unclear. P2Ox was found to be encoded by only one gene in the *P. chrysosporium* genome, therefore the co-purification of closely related isoforms can reasonably be ruled out. A possible explanation for this heterogeneity of the enzyme preparation from the natural, fungal source could be partial degradation by endogenous proteases or by proteases that are released from autolysing fungal mycelium during prolonged cultivation. Here, the expression in *E. coli* is certainly of advantage since proteolytic modification can be largely avoided by short cultivation times and low-protease expression hosts.

Previous attempts at determining the N-termini of purified pyranose oxidases have yielded ambiguous results, with the first amino acid obtained in sequencing being as far as 66 amino acid residues into the conceptual translations of the respective ORFs (Artolozaga et al., 1997; Nishimura et al., 1996; Takakura and Kuwata, 2003). It has been speculated that processing of P2Ox, i.e., removal of a putative (unidentified) signal sequence is responsible for these discrepancies (Nishimura et al., 1996; Takakura and Kuwata, 2003). Yet, this removal of parts of the N-terminal region is especially pronounced for *Pc*P2Ox isolated from its original fungal source, for which the N terminus QFGPGQVPIPGYSKNNEIEYQKDIDRFVNVI was reported (Artolozaga et al., 1997). This N-terminus starts at amino acid position 66 (Fig. 6), within a 22-amino acid insert not found in P2Ox of the *Trametes*/*Peniophora* group and only after the canonical ADP-binding βαβ motif xhxhGxGxxGxxxhxxh(x)$_8$hxhE(D), where x is any amino acid, and h is a hydrophobic residue, which is present in a large number of flavin and nicotinamide-dependent enzymes (Dym and Eisenberg, 2001; Wierenga et al., 1986). Proteolytic activity associated with ageing and partly autolysing mycelium as mentioned above could be a possible explanation. At present, it is not known how the removal of an essential part of the flavin-binding region as observed for *Pc*P2Ox isolated from its natural source is affecting the prop-

Fig. 6. Sequence coverage of recP2Ox (with T7-tag on N-terminus). Peptides identified by MS/MS sequencing are underlined, the native N-terminus is marked with an '↓', the N-terminus described in Artolozaga et al. (1997) is marked with an '×', canonical amino acids in the boxed ADP-binding βαβ-motif are in bold print.

erties of the enzyme, however, it was speculated that this might influence stability (De Koker et al., 2004). For P2Ox from *Trametes* spp. N-termini were described starting at amino acid 29 (Leitner et al., 2001), within a stretch of amino acids that is not present in, e.g., the *Phanerochaete* enzyme, and before the above-mentioned ADP-binding motif. Although suggestive of a signal sequence, neither the removed parts nor the cleavage sites conform to the respective established consensus motifs.

The activity profiles and kinetic properties of recP2Ox from *P. chrysosporium* described here are in excellent agreement with data that were reported previously for the native enzyme purified from its original source (e.g., fungal wild-type *Pc*P2Ox: $k_{cat,Glc} = 98.8\ s^{-1}$, $K_{m,Glc} = 1.09$ mM; recombinant *Pc*P2Ox: $k_{cat,Glc} = 83.1\ s^{-1}$, $K_{m,Glc} = 0.84$ mM) (Artolozaga et al., 1997; Volc and Eriksson, 1988), as well as on pyranose oxidases from related sources (Leitner et al., 2001; Takakura and Kuwata, 2003), indicating that the addition of the two tags does not interfere with the kinetic properties of the enzyme. A subject that has not been investigated to date is the ability of P2Ox from *P. chrysosporium* to utilize electron acceptors other than molecular oxygen. We have found that the recombinantly produced enzyme is indeed able to transfer very efficiently electrons derived from sugar oxidation onto alternative acceptors, both one- and two-electron acceptors. Some of these alternative electron acceptors studied for *Pc*P2Ox, including 1,4-benzoquinone or the ferricenium ion, are far better substrates than the presumed *in vivo* substrate oxygen (Artolozaga et al., 1997; Daniel et al., 1994), as judged by both the catalytic constant k_{cat} and the catalytic efficiency k_{cat}/K_m (Table 3). This latter bimolecular steady-state constant reached values of, e.g., $3.6–12 \times 10^6\ M^{-1}\ s^{-1}$ for 1,4-benzoquinone, $2.15 \times 10^6\ M^{-1}\ s^{-1}$ for the benzoquinone imine DCIP, or $0.69–1.9 \times 10^6\ M^{-1}\ s^{-1}$ for Fc^+, an organically complexed iron, indicating very rapid and efficient catalysis, also in comparison with oxygen showing a k_{cat}/K_m of $0.87 \times 10^6\ M^{-1}\ s^{-1}$ (Artolozaga et al., 1997). These data are in excellent accordance with those obtained for the only other P2Ox studied pertaining to its activity with alternative electron acceptors, P2Ox from *T. multicolor* (Leitner et al., 2001), which also showed higher activity with several one- and two-electron acceptors, most prominently various quinoid substrates, than with oxygen. The introduction of various substituents at position 2 of 1,4-benzoquinone resulted in a dramatic decrease of the catalytic efficiency of *Pc*P2Ox mainly by affecting k_{cat}, regardless whether an electron-withdrawing or an electron-donating group was introduced. A correlation between the reactivity of electron acceptors and their redox potential was also not possible. For example, 2-chloro-1,4-benzoquinone has a redox potential that is comparable to that of 1,4-benzoquinone [$E(Q/QH_2)$ of 0.304 and 0.298 V versus SHE, respectively (Cape et al., 2006), yet a k_{cat} that is lower by three orders of magnitude. The one-electron acceptors Fc^+, ABTS cation radical and ferricyanide have high redox potentials ($E^{0'}$ of 0.430, 0.520 and 0.358 V, respectively). Fc^+ is an excellent substrate of P2O with a catalytic efficiency of $691\ mM^{-1}\ s^{-1}$ at pH 6.5, while both the ABTS cation radical and ferricyanide are reduced significantly slower (13.4 and $0.087\ mM^{-1}\ s^{-1}$).

Based on the reactivity with alternative electron acceptors and the kinetic data determined it seems plausible that pyranose oxidase not only utilizes oxygen under natural conditions but also various quinones resulting from lignin metabolism and/or complexed metal ions as its substrates. Variously substituted benzoquinones are generated by the peroxidase-catalyzed oxidation of lignin, and are intermediates in the degradation of aromatic compounds by wood-decay fungi, as recently reviewed (Martinez et al., 2005). These benzoquinones are reduced to hydroquinones and undergo further intracellular metabolism. A 1,4-benzoquinone reductase, which is an FMN-containing flavoprotein using NAD(P)H as its second substrate, has been proposed for this activity in intracellular aromatic metabolism (Akileswaran et al., 1999; Brock and Gold, 1996; Brock et al., 1995). Alternatively, extracellular redox cycling of quinones may contribute to the generation of reactive oxygen species (ROS) for non-enzymatic attack of lignocellulose (Hammel et al., 2002). The periplasmic location of P2Ox (or even extracellular under certain growth conditions), together with the quinone reducing activity as demonstrated here, suggests that the oxidase could play a role in this extracellular metabolism.

An analysis of the *Pc*P2Ox amino acid sequence as derived from the coding sequence of the encoding gene as well as a comparison with P2Ox sequences from other sources, including their phylogenetic relationships, has already been reported (De Koker et al., 2004). That study focused on identifying amino acid residues that are strictly conserved not only among pyranose 2-oxidase proteins but also throughout the GMC-family of flavin-dependant enzymes. The availability of the crystal structure of *T. multicolor* P2Ox complexed with its slow substrate 2-deoxy-2-fluoro-D-glucose allows a more detailed comparison focusing on certain amino acids in the immediate vicinity of the active site. T169 was postulated to form a hydrogen bond with the flavin's N_5–O_4 during the oxidative half-reaction, supporting the electron transfer to the acceptor (Kujawa et al., 2006), as well as partially accounting for the substrate specificity due to steric hindrances between the amino acid side chain and the axially oriented C4 hydroxyl group of D-galactose – the equatorially oriented C4 hydroxyl group of D-glucose can be better accommodated. Side chains of D452, an amino acid of the active-site loop, and R472 are postulated to form hydrogen bonds with the O6 of the substrate, with additional hydrogen bonds being formed by Q448 and V546, while H548 and N593 putatively control the catalytic event by supporting the electron transfer from the substrate C2 (or C3) to the N5 of the flavin. The alignment of several P2Ox amino acid sequences as reported previously (De Koker et al., 2004) shows the conservation of all these amino acids in *Pc*P20x (Q448/Q454, R472/R478 and N593/N596) as well as their immediate vicinities, such as the motif THWTC (166–170 in *Tm*P20x, 157–161 in *Pc*P20x, containing the flavin-anchoring residue H167/H158) and the active site loop DAFSYG (452–457 in *Tm*P20x, 458–463 in *P. chrysosporium*). The only exception is V546 (the valine at this position is common in *Trametes* and *Peniophora* sequences), which corresponds to A551 in *P. chrysosporium* and A538 in *L. shimeiji*. In *Tm*P20x, V546 is interacting with the C1 hydroxyl group of the bound sugar substrate by forming a hydrogen bond through its carbonyl oxygen rather than interacting through its side chain, hence an alanine at this position should not alter the function of this active site residue. This high overall similarity with respect to the active site and to amino acids that were identified as crucial for substrate binding and oxidation is reflected in the catalytic properties of *Pc*P2Ox, which do not dramatically differ from *Tm*P2Ox, as mentioned above.

We have also searched the genomes of other fungi for the presence of P2Ox-encoding genes, including *Laccaria bicolor*, *Postia placenta* (both at http://genome.jgi-psf.org/) and *Coprinopsis cinerea* (http://fungal.genome.duke.edu/). *Laccaria* (Agaricales, Tricholomataceae) is an ectomycorrhizal symbiotic fungus (Martin et al., 2008); *Postia* (Polyporales, Coriolaceae) is physiologically classified as a wood-degrading brown-rot fungus, which selectively degrades cellulose while leaving the lignin fraction largely untouched (Wei et al., 2008), whereas *Coprinopsis* is a litter-decomposing fungus belonging to the Agaricales (Psathyrellaceae). No genes encoding enzymes with significant similarities to the P2Ox amino acid sequence could be identified in these genomes. This is in agreement with a previous study (Volc et al., 2001) where 76 basidiomycetous fungi were screened for activity of P2Ox and/or the catalytically and structurally related pyranose dehydrogenase (PDH, (Kujawa et al., 2007; Sygmund et al., 2007)). The authors reported PDH to be limited to litter-decomposing Agaricaceae and Lycoperdaceae (*C.*

cinerea is a close relative), whereas P2Ox was only produced by the white-rot fungi included in the study. Several fungi produced neither activity under the conditions tested. It has to be noted, however, that there is a number of oxidoreductases with similar catalytic activities and conceivably similar or overlapping biological functions *in vivo,* such as aryl alcohol oxidases or cellobiose dehydrogenases, many of which show significant sequence similarities with each other. The *C. cinerea* genome contains a number of similar genes encoding such putative oxidoreductases, which are not experimentally confirmed or catalytically characterized to date (Kittl et al., 2008). Phylogenetically, all known *p2ox* genes are descendants of a *Firmicutes* gene encoding a 2-keto-gluconate dehydrogenase (GenBank accession AAY60294), suggesting horizontal gene transfer from *Firmicutes* (Kittl et al., 2008). In this context it is interesting to note that a gene in the genome of the phylogenetically distant ascomycete *Aspergillus nidulans* was annotated to encode a pyranose 2-oxidase (glucose 2-oxidase, protein accession no. Q5B2E9). This indicates a rather early transfer event, after which the introduced gene has "survived" in a number of phylogenetically diverse groups, but was lost in others – there are species with and without *p2ox* genes among the Tricholomataceae as well as the Coriolaceae – as well as an evolution of these genes to eventually fulfil diverse biological functions in physiologically diverse fungi such as *A. nidulans*, which does not degrade lignocellulose.

References

Akileswaran, L., Brock, B.J., Cereghino, J.L., Gold, M.H., 1999. 1,4-Benzoquinone reductase from *Phanerochaete chrysosporium*: cDNA cloning and regulation of expression. Appl. Env. Microbiol. 65, 415–421.

Artolozaga, M.J., Kubátová, E., Volc, J., Kalisz, H.M., 1997. Pyranose 2-oxidase from *Phanerochaete chrysosporium* – further biochemical characterisation. Appl. Microbiol. Biotechnol. 47, 508–514.

Ausubel, F.M., Brent, R., Kingston, R.E., Moore, D.D., Seidman, J.G., Smith, J.A., Struhl, K., 1990. Current Protocols in Molecular Biology. Wiley Interscience, New York.

Bannwarth, M., Bastian, S., Heckmann-Pohl, D., Giffhorn, F., Schulz, G.E., 2004. Crystal structure of pyranose 2-oxidase from the white-rot fungus *Peniophora* sp. Biochemistry 43, 11683–11690.

Bastian, S., Rekowski, M.J., Witte, K., Heckmann-Pohl, D.M., Giffhorn, F., 2005. Engineering of pyranose 2-oxidase from *Peniophora gigantea* towards improved thermostability and catalytic efficiency. Appl. Microbiol. Biotechnol. 67, 654–663.

Baute, M.-A., Baute, R., Deffieux, G., Filleau, M.-J., 1977. Conversion of glucose to cortalcerone via glucosone by *Corticium caeruleum*. Phytochemistry 16, 1895–1897.

Bornscheuer, U.T., Pohl, M., 2001. Improved biocatalysts by directed evolution and rational protein design. Curr. Opin. Chem. Biol. 5, 137–143.

Brock, B.J., Gold, M.H., 1996. 1,4-Benzoquinone reductase from the basidiomycete *Phanerochaete chrysosporium*: spectral and kinetic analysis. Arch. Biochem. Biophys. 331, 31–40.

Brock, B.J., Rieble, S., Gold, M.H., 1995. Purification and characterization of a 1 4-benzoquinone reductase from the basidiomycete *Phanerochaete chrysosporium*. Appl. Env. Microbiol. 61, 3076–3081.

Cape, J.L., Bowman, M.K., Kramer, D.M., 2006. Computation of the redox and protonation properties of quinones: towards the prediction of redox cycling natural products. Phytochemistry 67, 1781–1788.

Christensen S., Lassen S.F., Schneider P., Nucleic acid encoding polypeptides having pyranose oxidase activity. US Patent 6,146,865 (2000).

Daniel, G., Volc, J., Kubatova, E., 1994. Pyranose oxidase, a major source of H_2O_2 during wood degradation by *Phanerochaete chrysosporium*, *Trametes versicolor*, and *Oudemansiella mucida*. Appl. Env. Microbiol. 60, 2524–2532.

Daniel, G., Volc, J., Kubatova, E., Nilsson, T., 1992. Ultrastructural and immunocytochemical studies on the H_2O_2-producing enzyme pyranose oxidase in *Phanerochaete chrysosporium* grown under liquid culture conditions. Appl. Env. Microbiol. 58, 3667–3676.

Danneel, H.-J., Ullrich, M., Giffhorn, F., 1992. Goal-oriented screening method for carbohydrate oxidases produced by filamentous fungi. Enzyme Microb. Technol. 14, 898–903.

De Koker, T.H., Mozuch, M.D., Cullen, D., Gaskell, J., Kersten, P.J., 2004. Isolation and purification of pyranose 2-oxidase from *Phanerochaete chrysosporium* and characterization of gene structure and regulation. Appl. Environ. Microbiol. 70, 5794–5800.

Dym, O., Eisenberg, D., 2001. Sequence-structure analysis of FAD-containing proteins. Protein Sci. 10, 1712–1728.

Eriksson, K.-E., Pettersson, B., Volc, J., Musilek, V., 1986. Formation and partial characterization of glucose-2-oxidase, a H_2O_2 producing enzyme in *Phanerochaete chrysosporium*. Appl. Microbiol. Biotechnol. 23, 257–262.

Freimund, S., Huwig, A., Giffhorn, F., Köpper, S., 1998. Rare keto-aldoses from enzymatic oxidation: Substrates and oxidation products of pyranose 2-oxidase. Chem. Eur. J. 4, 2442–2455.

Giffhorn, F., 2000. Fungal pyranose oxidases: occurrence, properties and biotechnical applications in carbohydrate chemistry. Appl. Microbiol. Biotechnol. 54, 727–740.

Hallberg, B.M., Leitner, C., Haltrich, D., Divne, C., 2004. Crystal structure of the 270 kDa homotetrameric lignin-degrading enzyme pyranose 2-oxidase. J. Mol. Biol. 341, 781–796.

Hammel, K.E., Kapich, A.N., Jensen Jr., K.A., Ryan, Z.C., 2002. Reactive oxygen species as agents of wood decay by fungi. Enzyme Microb. Technol. 30, 445–453.

Heckmann-Pohl, D.M., Bastian, S., Altmeier, S., Antes, I., 2006. Improvement of the fungal enzyme pyranose 2-oxidase using protein engineering. J. Biotechnol. 124, 26–40.

Kittl, R., Sygmund, C., Halada, P., Volc, J., Divne, C., Haltrich, D., Peterbauer, C.K., 2008. Molecular cloning of three pyranose dehydrogenase-encoding genes from *Agaricus meleagris* and analysis of their expression by real-time RT-PCR. Curr. Genet. 53, 117–127.

Kotik, M., Kocanova, M., Maresova, H., Kyslik, P., 2004. High-level expression of a fungal pyranose oxidase in high cell-density fed-batch cultivations of *Escherichia coli* using lactose as inducer. Protein Expr. Purif. 36, 61–69.

Kujawa, M., Ebner, H., Leitner, C., Hallberg, B.M., Prongjit, M., Sucharitakul, J., Ludwig, R., Rudsander, U., Peterbauer, C., Chaiyen, P., Haltrich, D., Divne, C., 2006. Structural basis for substrate binding and regioselective oxidation of monosaccharides at C3 by pyranose 2-oxidase. J. Biol. Chem. 281, 35104–35115.

Kujawa, M., Volc, J., Halada, P., Sedmera, P., Divne, C., Sygmund, C., Leitner, C., Peterbauer, C., Haltrich, D., 2007. Properties of pyranose dehydrogenase purified from the litter-degrading fungus *Agaricus xanthoderma*. FEBS J. 274, 879–894.

Leitner, C., Volc, J., Haltrich, D., 2001. Purification and characterization of pyranose oxidase from the white rot fungus *Trametes multicolor*. Appl. Env. Microbiol. 67, 3636–3644.

Maresova, H., Vecerek, B., Hradska, M., Libessart, N., Becka, S., Saniez, M.H., Kyslik, P., 2005. Expression of the pyranose 2-oxidase from *Trametes pubescens* in *Escherichia coli* and characterization of the recombinant enzyme. J. Biotechnol. 120, 387–395.

Martin, F., Aerts, A., Ahren, D., Brun, A., Danchin, E.G.J., Duchaussoy, F., Gibon, J., Kohler, A., Lindquist, E., Pereda, V., Salamov, A., Shapiro, H.J., Wuyts, J., Blaudez, D., Bue, M., Brokstein, P., Canback, B., Cohen, D., Courty, P.E., Coutinho, P.M., Delaruelle, C., Detter, J.C., Deveau, A., Difazio, S., Duplessis, S., Fraissinet-Tachet, L., Lucic, E., Frey-Klett, P., Fourrey, C., Feussner, I., Gay, G., Grimwood, J., Hoegger, P.J., Jain, P., Kilaru, S., Labbe, J., Lin, Y.C., Legue, V., Le Tacon, F., Marmeisse, R., Melayah, D., Montanini, B., Muratet, M., Nehls, U., Niculita-Hirzel, H., Peter, M., Quesneville, H., Rajashekar, B., Reich, M., Rouhier, N., Schmutz, J., Yin, T., Chalot, M., Henrissat, B., Kües, U., Lucas, S., Van De Peer, Y., Podila, G.K., Polle, A., Pukkila, P.J., Richardson, P.M., Rouze, P., Sanders, I.R., Stajich, J.E., Tunlid, A., Tuskan, G., Grigoriev, I.V., 2008. The genome of *Laccaria bicolor* provides insights into mycorrhizal symbiosis. Nature 452, 88–92.

Martinez, A.T., Speranza, M., Ruiz-Duenas, F.J., Ferreira, P., Camarero, S., Guillen, F., Martinez, M.J., Gutierrez, A., Del Rio, J.C., 2005. Biodegradation of lignocellulosics: microbial, chemical, and enzymatic aspects of the fungal attack of lignin. Int. Microbiol. 8, 195–204.

Martinez, D., Larrondo, L.F., Putnam, N., Sollewijn Gelpke, M.D., Huang, K., Chapman, J., Helfenbein, K.G., Ramaiya, P., Detter, J.C., Larimer, F., Coutinho, P.M., Henrissat, B., Berka, R., Cullen, D., Rokhsar, D., 2004. Genome sequence of the lignocellulose degrading fungus *Phanerochaete chrysosporium* strain RP78. Nat. Biotechnol. 22, 695–700.

Nishimura, I., Okada, K., Koyama, Y., 1996. Cloning and expression of pyranose oxidase cDNA from *Coriolus versicolor* in *Escherichia coli*. J. Biotechnol. 52, 11–20.

Shin, K.S., Youn, H.D., Han, Y.H., Kang, S.O., Hah, Y.C., 1993. Purification and characterization of D-glucose-oxidase from white-rot fungus *Pleurotus ostreatus*. Eur. J. Biochem. 215, 747–752.

Stevens, R.C., 2000. Design of high-throughput methods of protein production for structural biology. Structure 8, R177–R185.

Stewart, P., Cullen, D., 1999. Organization and differential regulation of a cluster of lignin peroxidase genes of *Phanerochaete chrysosporium*. J. Bacteriol. 181, 3427–3432.

Sygmund, C., Kittl, R., Volc, J., Halada, P., Kubatova, E., Haltrich, D., Peterbauer, C.K., 2007. Characterization of pyranose dehydrogenase from *Agaricus meleagris* and its application in the C-2 specific conversion of D-galactose. J. Biotechnol. 133, 334–342.

Takakura, Y., Kuwata, S., 2003. Purification, characterization, and molecular cloning of a pyranose oxidase from the fruit body of the basidiomycete *Tricholoma matsutake*. Biosci. Biotechnol. Biochem. 67, 2598–2607.

Tasca, F., Timur, S., Ludwig, R., Haltrich, D., Volc, J., Antiochia, R., Gorton, L., 2007. Amperometric biosensors for detection of sugars based on the electrical wiring of different pyranose oxidases and pyranose dehydrogenases with osmium redox polymers on graphite electrodes. Electroanalysis 19, 294–302.

Vecerek, B., Maresova, H., Kocanova, M., Kyslik, P., 2004. Molecular cloning and expression of the pyranose 2-oxidase cDNA from *Trametes ochracea* MB49 in *Escherichia coli*. Appl. Microbiol. Biotechnol. 64, 525–530.

Volc, J., Eriksson, K.-E., 1988. Pyranose 2-oxidase from *Phanerochaete chrysosporium*. Methods Enzymol. 161, 316–322.
Volc, J., Kubatova, E., Daniel, G., Sedmera, P., Haltrich, D., 2001. Screening of basidiomycete fungi for the quinone-dependent sugar C-2/C-3 oxidoreductase, pyranose dehydrogenase, and properties of the enzyme from *Macrolepiota rhacodes*. Arch. Microbiol. 176, 178–186.
Wei, Y.L., Dai, Y.C., Wang, L., Zuo, H.W., 2008. A preliminary study on ecology of wood brown-rot fungi of *Postia*. Forest Res. 21, 55–59.
Wierenga, R.K., Terpstra, P., Hol, W.G.J., 1986. Prediction of the occurrence of the ADP-binding βαβ-fold in proteins, using an amino acid sequence fingerprint. J. Mol. Biol. 187, 101–107.